Research Article

Alaa H. J. Al-Rkaby*, Noor Aamer Odeh, Ahmed Sabih, and Haider Odah

Geotechnical characterization of sustainable geopolymer improved soil

https://doi.org/10.1515/jmbm-2022-0044
received February 28, 2022; accepted April 09, 2022

Abstract: Geopolymer (GP) has recently emerged as a novel and environmental friendly alternative to conventional soil stabilization products like lime and Ordinary Portland Cement (OPC), which adversely affect the environment. This article emphasizes GPs produced from high calcium class C fly ash (CFA) and an alkali activator comprising sodium hydroxide and sodium silicate solution for sand stabilization. The experimental program includes a series of unconfined compressive strength (UCS), flexural strength, tensile strength, and microstructural analyses using scanning electron microscopy. Results revealed that UCS, flexural strength, and tensile strength of GP-treated soil were in the range of 2–10, 0.5–2.0, and 0.4–1.2 MPa, respectively (depending on the ratio of fly ash and activator). These strengths were even higher than those of cement-stabilized soil. The microstructural analysis revealed that the formation of dense calcium–sodium alumina–silicate hydrated gel (C, N–A–S–H) is the reason for strength improvement. According to the findings of this study, using a CFA-GP binder for soil improvement is a viable alternative to OPC in geotechnical applications.

Keywords: class C fly ash, UCS, indirect strength, flexural strength, geopolymer, sand soil, SEM/EDS

1 Introduction

Several essential engineering properties of soils can be beneficially modified by chemical treatment using traditional binders (*e.g.*, lime and cement). However, during the last decade, the carbon footprint associated with such binders has had greater significant environmental problems. Ordinary Portland Cement (OPC) production is predicted to be around 7% of total artificial carbon dioxide emission [1]. Considering this emission issue and other inevitable environmental negative consequences associated with nonrenewable raw materials, there is a motivation to develop more ecologically cost-effective and friendly alternative binders to replace OPC. As a result, special attention has been focused on the valuable recycling process materials from aluminosilicate industrial wastes and through alkali-activated cement [2]. Geopolymers (GPs) are cementitious binders produced from industrial byproducts, and the waste has great amorphous (Si and Al) content, like fly ash (FA) and metakaolin (MK), with an alkaline activator (such as potassium/sodium silicate and potassium/sodium hydroxide) [3]. Geopolymerization is a four-stage chemical reaction that occurs rapidly: (i) ion dissolution, (ii) ion diffusion, (iii) gel development by polymerization of Si and Al compounds with an activator, and (iv) gel hardening, [4]. Depending on the conditions under which they are synthesized, GP may have excellent mechanical qualities such as high strength, low permeability, high durability, and minor volume changes [5]. However, various parameters, such as the rate of the source materials, the chemical properties of the activator, temperature, and curing time, may influence the mechanical properties of GP. Among these parameters, the curing temperature is the most difficult to apply in the field [4,5].

GPs are typically treated at temperatures 60–90°C; therefore, most GPs have been confined to usage in dry heat-cured or steamed concrete [6]. GPs must be used at room temperature for geotechnical engineering applications since treating them at high temperatures is impractical. The rate of geopolymerization is significantly slower at low temperatures than at higher temperatures; thus, the impact strength of GP-soil is lower and occurs over a longer timescale than cement-treated soil [7]. Therefore, high activator concentrations are required to enhance the practicality and effectiveness of GPs based on FA compared to cement for stabilizing soil applications. On the other hand, using activator content in bulk raises the

* **Corresponding author: Alaa H. J. Al-Rkaby,** College of Engineering, University of Thi-Qar, Nasiriyah, Iraq,
e-mail: alaa.astm@gmail.com, alaa.al-rakaby@utq.edu.iq
Noor Aamer Odeh, Ahmed Sabih, Haider Odah: College of Engineering, University of Thi-Qar, Nasiriyah, Iraq

total cost of this stabilization approach [8]. So far, the research on FA GP has relied on a precursor obtained from class F fly ash (FFA) produced by the combustion of bituminous coals [9]. To reduce the desired amount of activator ratio (*i.e.*, increase cost effectiveness) while maintaining adequate curing at room temperature, this study focused on improving the reactivity of the GP by using FA with high Ca content. The main difference between FFA and class C fly ash (CFA) in terms of composition is the calcium concentration. Still, both often include significant quantities of silica and alumina. CFA has a composition between ground-granulated blast-furnace slag (GGBFS) and FFA [10]. The fact that the mixes of GGBFS and FFA are often preferred in the production of GP also indicates the potential of CFA for producing GP.

It has been noticed that a lot of research on GP-stabilized soils published in the literature is primarily concerned with increasing the compressive strength of treated soils [4,9–12]. However, the tensile and flexural performance of GP-treated soil has not been considered extensively. Tensile and flexural stresses can develop in earth structures, especially in the pavement, in the earth, and earth-rock fill dams, where the stresses may cause failures of such structures. In this research, the mechanical properties of GP-stabilized sand soil will be investigated using high calcium CFA, including unconfined compressive strength (UCS), tensile, and flexural strength tests, compared with the traditional OPC at high binder dosage. In addition, the microstructural advancement of soil- FA GP was investigated using scanning electron microscopy (SEM) analysis.

2 Materials and methodology

2.1 Soil

The dry sand used in this research was locally available and was classified as SP by unified soil classification system. Figure 1 depicts the grain size distribution of the soil. Table 1 provides a summary of the physical characteristics of the soil.

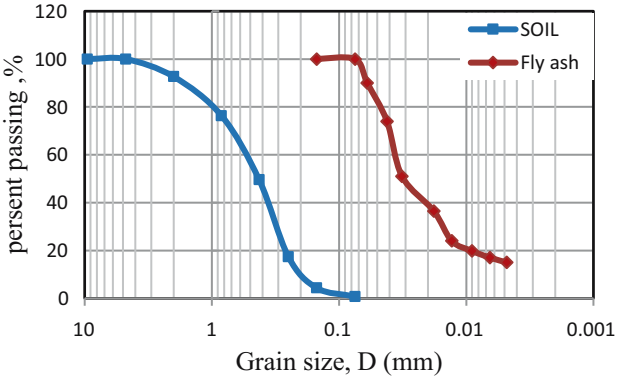

Figure 1: Grain size distribution curve of sand and FA.

2.2 GP ingredients

This study used a mixture of FA and liquid-based sodium activator (referred herein as AC) as the GP binder. FA was obtained from coal-fired power plants. Figure 1 depicts the particle distribution as determined by the hydrometer test. In addition, the chemical compositions that energy dispersive spectroscopy (EDS) analyzed are presented in Table 2. FA could be classified into high calcium CFA based on its chemical composition specified in ASTM standard C618, where it can be noted that its contents Al_2O_3, SiO_2, and Fe_2O_3 are >50%, and Ca content is higher than 10%. Figure 2 shows images of FA taken with a scanning electron microscope at high resolution. The micrograph reveals that the FA consists of spherical particles of various sizes. The activator from a mix of sodium hydroxide (NaOH) and sodium silicate (Na_2SiO_3) was used in this study. Before mixing with Na_2SiO_3, NaOH was dissolved in distilled water for at least 24 h at a molar concentration of 10 M. The mass ratio of Na_2SiO_3/NaOH was set to 2.0 to create a maximized early strength and a massive alkaline environment.

2.3 Sample preparation

To prepare a specimen for all the tests, the mixing procedure was the same:

1. To ensure mixture uniformity, the source material (FA) was mixed as a partial replacement (by weight) with dry soil for 5 min in ratios of 10, 15, and 20% (*i.e.*, to

Table 1: Physical properties of soil

Soil property	Uniformity coefficient (Cu)	Coefficient of curvature (Cc)	Mean effective diameter (D50)	Specific gravity (Gs)	Maximum dry unit weight (g/cm³)	Minimum dry unit weight (g/cm³)	Internal friction angle (φ°)
Value	3	0.89	0.44	2.65	1.701	1.439	36

Table 2: EDS analysis of FA chemical compositions

Elt	Concentration by % weight										
	C	O	F	Na	Mg	Al	Si	S	K	Ca	Fe
FA	1.01	12.71	0	2.72	2.8	19.18	37.65	1.6	1.5	21.11	4.09

stabilize 100 g of dry soil with FA 10%, 10 g of dry FA is mixed with 90 g of soil).

2. Alkali activator was created by combining a sufficient quantity of NaOH and Na_2SiO_3 based on the alkaline proportions of the mixes for 5 min and leaving it at room temperature for an additional 5–10 min.
3. The alkaline solution is mixed in various ratios (AC/FA 0.4, 0.6) with free water to achieve the required water content and then gradually added to the dry mixture for an additional 3–5 min. The various ingredients were mixed until a homogeneous mixture was obtained. Table 3 summarizes the details of the mixtures used.
4. To achieve the desired density, the final mixture was compacted in controlled weight/thickness layers for each sample.
5. After compaction, the GP sample was kept for 24 h before being soaked in water for 28 days to cure.
6. To compare the GP-stabilized samples with the soil-cement samples, additional samples were prepared and stabilized by adding 5% OPC, as shown in Table 3.

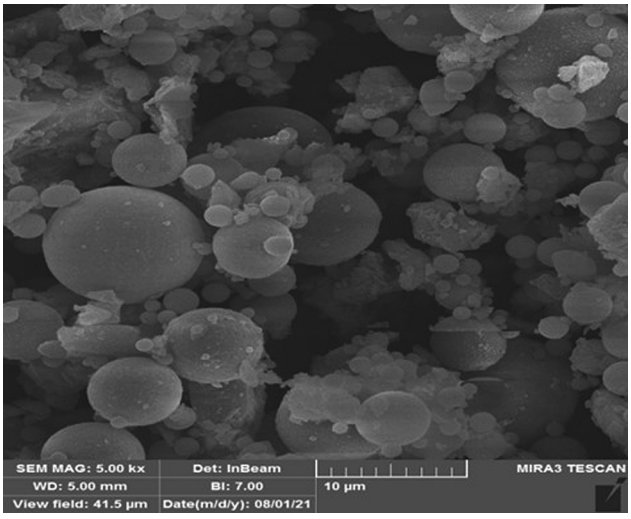

Figure 2: SEM image of FA.

2.4 Tests conducted

2.4.1 UCS

UCS tests were carried out after a 28-day curing period. The UCS test specimens were produced with 100 mm height (h) and 50 mm diameter (d) cylindrical split tubes made of PVC with an h:d aspect ratio of 2:1, as specified by ASTM D1633-00, 2007 [13]. UCS test for samples was performed using a uniaxial machine with a loading capacity of 50 kN, at a displacement rate of 0.1 mm/min.

2.4.2 Flexural strength

Three-point bending tests were performed on specimens according to ASTM 1635/D1635M-19, 2019. Treated specimens were molded in rectangular molds with dimensions of 35, 35, 130 mm and tested after 28 days of curing. Flexural strength of samples was calculated using the following equation:

$$\text{fs} = \frac{3Pl}{2bd^2}, \tag{1}$$

where fs is the flexural strength (MPa), l is the span of the simple supports (mm), P is the max load (N), b is the width of the sample (mm), and d is the thickness of the sample (mm).

Table 3: Details of mixtures used

Sample[a]	%FA[b]	AC/FA[c]	OPC
S-F10A0.4	10	0.4	—
S-F15A0.4	15	0.4	—
S-F20AO.4	20	0.4	—
S-F10AO.6	10	0.6	—
S-F15A0.6	15	0.6	—
S-F20A0.6	20	0.6	—
S-OPC	—	—	5

[a]Sample codes: S, sand; F, fly ash content; and A is an activator/fly ash ratio. [b]The fly ash percent. [c]Activator/fly ash ratio.

2.4.3 Indirect tensile strength (ITS)

The tensile strength of GP-treated soils was investigated using ITS tests on specimens after curing for 28 days. Cylindrical split tubes (PVC) with an h and d of 100 and 50 mm were used to create test samples. A uniaxial machine with a loading capacity of 50 kN and a displacement rate of 1 mm/min was used for the testing. The indirect tensile tests were performed according to Brazilian standard NBR 7222 [14]. The load is continuously applied from the top horizontal side of the cylinders until the maximum load is achieved. The peak load was measured, and the ITS was computed using the following formula:

$$\mathrm{St} = \frac{2P}{\pi h d}, \tag{2}$$

where St is the indirect tensile strength (MPa), d is the diameter, h is the height of the specimen in millimeters (mm), and P is the maximum load (N).

2.4.4 Microstructural analysis

SEM-EDS was used to investigate the microstructural advancement of gel structure and the change in soil texture after stabilization of fragments resulting from the broken specimens tested by the uniaxial machine. Fractured samples were coated with gold and analyzed using FE-SEM device (ARYA Electron Optic). Analyses were performed with a secondary electron detector with 15 kV acceleration voltage for image and 20 kV for EDS.

3 Results and discussion

3.1 UCS

Figure 3 demonstrates the impact of GP and cement addition on the stress–strain performance of sand soil as determined by UCS. In general, GP-treated soils were brittle yielding, with stress reaching a peak before an abrupt failure. Yielding was linked to a stiffer reaction as the GP ratio improved (*i.e.*, low strain and higher UCS), similar to the results offered in [13,14]. Although GP samples exhibited brittle stress–strain reaction, the samples were different in the axial strain and peak stress, particularly of the SI-F20A0.6 specimen, displayed the highest stress without a post-peak, implying an extremely brittle reaction.

The production of cementitious products is responsible for qualitative and quantitative change in the stress–strain response of stabilized soil. The activator's high pH levels dissolve the alumina and silica oxides from the FA particles inside the GP, resulting in a GP gel product that solidifies over time and cements the soil particles [10,15]. Also, it can be seen from the figure that the samples treated with GP had greater UCS than the cement-treated specimens (except for the samples mixed with FA = 10%). This is due to the presence of more pozzolanic and geopolymeric reactions in GP-treated mixes, as opposed to OPC-treated samples, which solely have pozzolanic reactions. In other words, the formation rate of cementitious products in the GP-soil is greater than that of the cement-soil. These findings align with the results in [15–18].

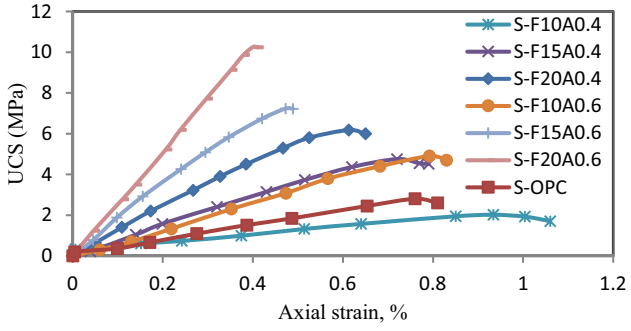

Figure 3: Unconfined stress–strain behavior.

3.2 Fs

The different mixtures for GP-soil created with various binder contents were tested for flexural strength. When flexural loading was applied to a soil beam, similar to concrete, flexural stress developed, resulting in fractures when the carrying strength of the soil was outperformed. In general, no plastic behavior was seen in any of the specimens. Instead, the load developed linearly with the deflection until fracture. Finally, failure occurred when a fracture developed at the bottom of the beam owing to stress. Then, as seen in Figure 4, it expanded up through the beam thickness until the beams cracked.

Figure 4: Crack development in a GP-soil beam under flexural loading.

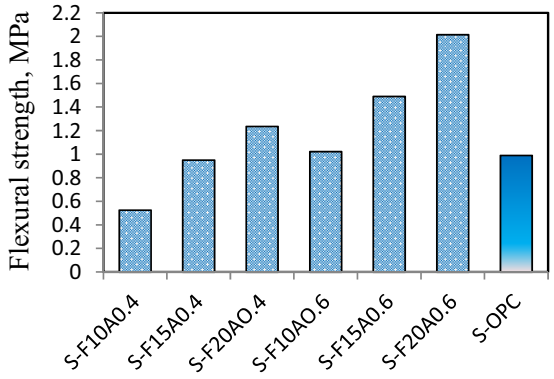

Figure 5: Flexural strength.

Figure 5 shows the relationship between the flexural strength of mixtures soil-cement and the soil-GP prepared with a percentage of AC/FA 0.4, 0.6 and FA 10, 15, and 20%. It can be observed from the results a pattern similar to that of the UCS results, the increase in GP content due to increased flexural strength. With the increase of AC/FA from 0.4 to 0.6, the flexural strength increases from 0.526, 0.95, and 1.26 MPa to 1.02, 1.49, and 2.01 MPa at FA 10, 15, and 20%, respectively.

When comparing the flexural strength of GP and cement-treated soil mixture, the flexural strength of GP specimens was higher than that of cement-treated samples. When the beams were subjected to flexural testing, both compression and tension stresses are induced under the applied load. However, beam failed clearly in the tension because the material is weaker in tension than in compression [19]. Previous research had shown that when geopolymeric binders were employed in concrete, they had both lower and higher Fs when compared to cement, depending on the ratio and composition of source materials [20]. Cement-stabilized mixes have lower Fs than GP-stabilized mixtures, and cement mixes had lower tensile strength than GP mixes.

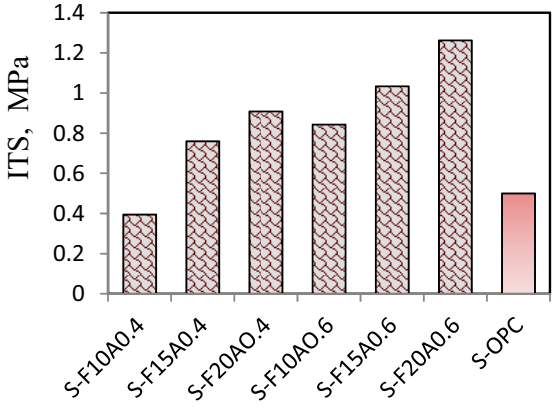

Figure 6: Indirect tensile strength.

3.3 ITS

The Brazilian indirect tensile test is often used to determine the tensile strength of rock masses or concrete. However, some researchers have effectively used it to assess the TS of cohesive soil [19–22]. Therefore, it should be feasible to determine the tensile strength for GP-soil. Figure 6 shows the graphical representation of GP and cement-treated soil mixtures. A pattern similar to compressive strength can be seen in the case of ITS. The tensile strength improves when the proportion of GP increases. When the ratio of FA is increased from 10 to 20%, the tensile strength is increased from 0.39 to 0.91 MPa (at AC/FA0.4) and from 0.84 to 1.2624 MPa (at AC/FA 0.6). Greater tensile strength for GP blends indicates a stronger cracking resistance, owing to the high stiffness of GP mixtures. This expectedly can be attributed to the presence of GP gel, which strengthens the bonding between the soil particles. As a result, the GP samples had a higher tensile strength.

A pattern similar to compressive strength and flexural strength can be seen that the tensile strength of the GP-stabilized mixtures is found to be greater than that of cement mixtures. Similar results were reported by Wang *et al.* [23], who investigated that the average ITS of MK-based GP enhanced soil is around 1.1 times that of cement soil.

3.4 Microstructural analysis

The structure of the FA-based GP is deduced primarily from the degradation of aluminum silicate in the FA by AC, which is the result of polycondensation. When an activator interacts with FA, the aluminosilicate bonds in FA are broken, resulting in the liberation of active Si^{4+} and Al^{3+}. These active Si^{4+} and Al^{3+} compose nuclei and aluminosilicate oligomers forming AlO_4 and SiO_4 tetrahedral structural [24]. Etching on FA surfaces, detected by SEM analysis, can reveal the rate of geopolymerization of FA [25].

As shown in Figure 7, SEM/EDS analysis was done on GP-soil specimens with varying AC and FA ratios. Micrographs of the 28-day age GP samples (S-F10A0.4 and S-F20A0.4) in Figure 7(a and b) show porous structures with partially reacted FA particles scattered in

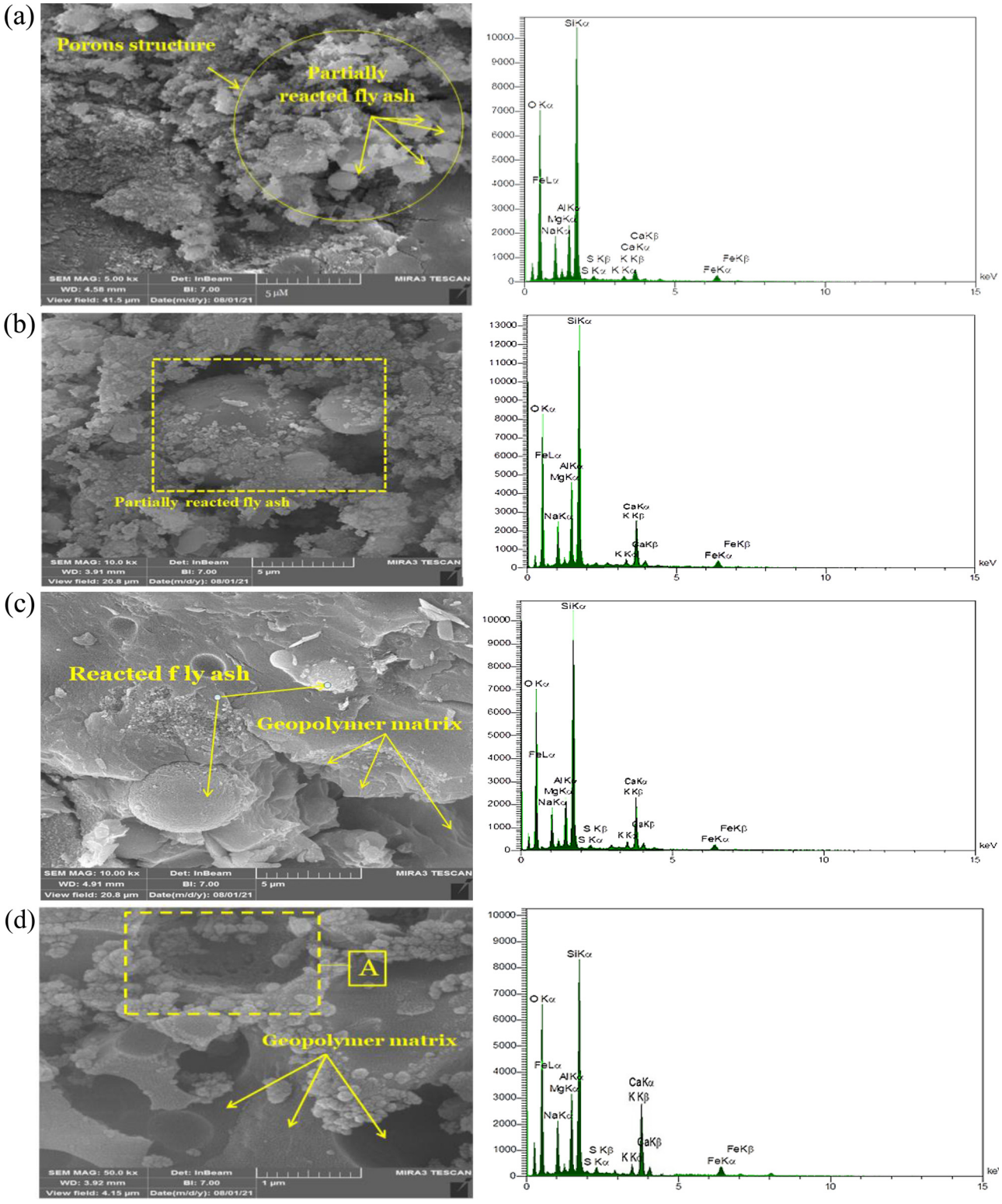

Figure 7: SEM-EDS result for soil-GP samples with different FA and AC ratios: (a) S-F10A0.4, (b) S-F20A0.4, (c) S-F15A0.6, and (d) S-F20A0.6.

GP gel. The reason may be that the activator is insufficient for the decomposition of silica and alumina with FA, resulting in GP gels that are not adequate for the binding of soil particles. However, the microstructure homogeneity improves with increasing dose of FA from 10 to 20% at the same alkaline activator (0.4), which explains

Table 4: Ratios of elements and chemical composition for soil-GP specimens

Mixture	FA%	AC/FA	Si	Al	Ca	Na	Si/Al	Ca/Si	Na/Al	UCS (MPa)
S-F10A0.4	10	0.4	30.5	7.45	2.98	7.57	4.1	0.1	1	2.21
S-F20A0.4	20	0.4	30.51	10.83	7.69	7.74	2.7	0.25	0.71	6.18
S-F15A0.6	15	0.6	27.3	9.32	10.3	8.51	2.82	0.38	0.91	7.32
S-F20A0.6	20	0.6	25.23	9.88	12.66	11.96	2.9	0.5	1.2	10.52

why the UCS of the sample (S-F20A0.4) increases. The "A" area in the sample (S-F20A0.6) in Figure 7(d) depicts the changes in the microstructure of a reactive FA sphere as a result of AC dissolution. The sphere seems shattered in the high alkaline state, and some of the Si–Al dissolve from the FA. Furthermore, the interior region of the fragmented FA appears to be loaded with a considerable number of reaction product microparticles.

Table 4 displays important proportions and compositions of the samples at 28 days. The main ratio of Si/Al is widely considered when the EDS technique is applied. More attention has been put on the elemental ratios of GPs in this issue to illustrate the link between these ratios and engineering characteristics. OPC and GP elemental ratios are generally 2.00–3.00 for Si/Al and 1.00 for Na/Al. Microstructures that are more dense, homogenous, and compact are formed when the Si/Al ratio increases. GP sample with a ratio of Si/Al = 2.92 (as sample S-F20A0.6) is extra homogeneous than with the ratio of Si/Al = 2.82, 2.7 (as samples S-F20A0.4 and S-F15A0.6). It is possible that this is related to the insoluble particles in FA. Interface connections with the binder formed by insoluble particles are sensitive regions. However, stable structures of (Si–O–Si) and Si species can be developed for greater ratio of Si/Al. This stability is achieved through a subsequent geopolymerization process, which results in a more complex network and homogeneous GP, resulting in increased strength. It can be noticed a decrease in UCS at Si/Al ratios = 4.1, as shown in the sample (S-F10A0.4). This corresponds to previous research. FA results in more heterogeneous matrices (*i.e.*, a more percentage of unreacted FA particles), with Si/Al ratios >3 [2]. From Table 4, it can also be seen that the Na/Al and Ca/Si ratios for all samples are in the ranges of 0.7–1.2 and 0.1–0.5. Related investigations found that the chemical percentages of alumina, silica, and calcium in GP were consistent [24,25]. As a result, the dominant geopolymeric gel was identified as (Na)-poly(sialate-disiloxo-), *i.e.*, Nan–(–Si–O–Al–O–Si–O–Si–O–Si–O–)*n*–. Geopolymeric gel, the major response product of FA, coexists with C, N–A–S–H gel and some unreacted spheres. This showed better performance compared with other types of stabilizers [26–33].

4 Conclusion

This study investigated the effectiveness of using GP based on CFA as a stabilizing technique for sand soils by conducting compression, tensile, and flexure strength tests on GP-treated and OPC-treated mixtures. Moreover, the microstructure of the select GP-treated mixtures was also examined by SEM analysis. The following conclusions were drawn from the results of the current experimental investigation:

1 – Under unconfined compression, the dominant stress–strain reaction for GP-soil was found to be a brittle yield, with the stress peaking before a sudden failure. When the GP ratio increases, the response becomes stiffer (*i.e.*, greater unconfined force and lower axial strain). In addition, the treated samples showed a higher UCS of GP than processed cement samples, which may be the result of the GP sample's combined geopolymeric and pozzolanic reactions.
2 – The flexural and tensile strength values are in the similar lines of compressive strength development. Results revealed that flexural and tensile strengths of GP-treated soil were in the range of 0.5–2.0 MPa and 0.4–1.2 MPa, respectively. These strengths were even higher than those of OPC-stabilized soil.
3 – The SEM analysis of soils stabilized by the GP revealed evidence of a progressive improvement in soil fabric homogeneity owing to GP gel formation, resulting in the creation of an enhanced rate of strength gain with increasing GP content.

Funding information: There was no specific grant for this research from any funding agency in the public, commercial, or not-for-profit sectors.

Author contributions: All authors have accepted full responsibility for the content of this manuscript and have given their approval for its submission.

Conflict of interest: Authors declare no conflict of interest

References

[1] Pacheco-Torgal F, Labrincha J, Leonelli C, Palomo A, Chindaprasit P. Handbook of alkali-activated cements, mortars and concretes. UK: Elsevier; 2014.

[2] Davidovits J. Geopolymer chemistry and applications. 2nd ed. Saint-Quentin, France: Institut Géopolymère; 2008.

[3] Singhi B, Laskar AI, Ahmed MA. Investigation on soil–geopolymer with slag, fly ash and their blending. Arab J Sci Eng. 2016;41(2):393–400. doi: 10.1007/s13369-015-1677-y.

[4] Zhang M, Guo H, El-Korchi T, Zhang G, Tao M. Experimental feasibility study of geopolymer as the next-generation soil stabilizer. Constr Build Mater. 2013;47:1468–78.

[5] Van Deventer JSJ, Xu H. Geopolymerisation of aluminosilicates: relevance to the minerals industry. Aus IMM Bull. 2002;33:20–7.

[6] Gianoncelli A, Zacco A, Struis RPWJ, Borgese L, Depero LE, Bontempi E. Fly ash pollutants, treatment and recycling. Pollut Dis Remediat Recycl. 2013;4:103–213.

[7] Cristelo N, Glendinning S, Miranda T, Oliveira D, Silva R. Soil stabilisation using alkaline activation of fly ash for self compacting rammed earth construction. Constr Build Mater. 2012;36:727–35.

[8] Bernal SA, Provis JL. Durability of alkali-activated materials: progress and perspectives. J Am Ceram Soc. 2014;97(4):997–1008.

[9] Phair JW, Van Deventer JSJ. Characterization of fly-ash-based geopolymeric binders activated with sodium aluminate. Ind Eng Chem Res. 2002;41(17):4242–51.

[10] Duxson P, Provis JL. Designing precursors for geopolymer cements. J Am Ceram Soc. 2008;91(12):3864–9.

[11] Cristelo N, Glendinning S, Miranda T, Oliveira D, Silva R. Soil stabilisation using alkaline activation of fly ash for self compacting rammed earth construction. Constr Build Mater. 2012;36:727–35. doi: 10.1016/j.conbuildmat.2012.06.037.

[12] Phummiphan I, Horpibulsuk S, Sukmak P, Chinkulkijniwat A, Arulrajah A, Shen S-L. Stabilisation of marginal lateritic soil using high calcium fly ash-based geopolymer. Road Mater Pavement Des. 2016;17(4):877–91.

[13] ASTM International. ASTM D1633-00(2007) standard test methods for compressive strength of molded soil–cement cylinders. West Conshohocken, PA, USA: ASTM International; 2007. p. 1–15. https://www.astm.org/DATABASE.CART/HISTORICAL/D1633-00.htm

[14] B. S. Association. Mortar and concrete – test method for splitting tensile strength of cylindrical specimens. NBR; 1983.

[15] Abdullah HH, Shahin MA, Walske ML. Geo-mechanical behavior of clay soils stabilized at ambient temperature with fly-ash geopolymer-incorporated granulated slag. Soils Found. 2019;59(6):1906–20. doi: 10.1016/j.sandf.2019.08.005.

[16] Yu J, Chen Y, Chen G, Wang L. Experimental study of the feasibility of using anhydrous sodium metasilicate as a geopolymer activator for soil stabilization. Eng Geol. 2020;264:105316.

[17] Yaghoubi M, Arulrajah A, Disfani MM, Horpibulsuk S, Bo MW, Darmawan S. Effects of industrial by-product based geopolymers on the strength development of a soft soil. Soils Found. 2018;58(3):716–28.

[18] Yip CK, Lukey GC, Van Deventer JSJ. The coexistence of geopolymeric gel and calcium silicate hydrate at the early stage of alkaline activation. Cem Concr Res. 2005;35(9):1688–97.

[19] Mbaraga AN, Jenkins KJ, van de Ven M. Influence of beam geometry and aggregate size on the flexural strength and elastic moduli of cement-stabilized materials. Transp Res Rec. 2014;2401(1):22–9.

[20] Nath P, Sarker PK. Flexural strength and elastic modulus of ambient-cured blended low-calcium fly ash geopolymer concrete. Constr Build Mater. 2017;130:22–31.

[21] Stirling RA, Hughes P, Davie CT, Glendinning S. Tensile behaviour of unsaturated compacted clay soils—a direct assessment method. Appl Clay Sci. 2015;112:123–33.

[22] Anggraini V, Huat BBK, Asadi A, Nahazanan H. Effect of coir fibers on the tensile and flexural strength of soft marine clay. J Nat Fibers. 2015;12(2):185–200. doi: 10.1080/15440478.2014.912973.

[23] Wang S, Xue Q, Zhu Y, Li G, Wu Z, Zhao K. Experimental study on material ratio and strength performance of geopolymer-improved soil. Constr Build Mater. 2020;267:120469. doi: 10.1016/j.conbuildmat.2020.120469.

[24] Zhuang XY, Chen L, Komarneni S, Zhou CH, Tong DS, Yang HM, et al. Fly ash-based geopolymer: clean production, properties and applications. J Clean Prod. 2016;125:253–67.

[25] Fernández-Jiménez A, Palomo A, Sobrados I, Sanz J. The role played by the reactive alumina content in the alkaline activation of fly ashes. Microporous Mesoporous Mater. 2006;91(1–3):111–9.

[26] Ahmari S, Ren X, Toufigh V, Zhang L. Production of geopolymeric binder from blended waste concrete powder and fly ash. Constr Build Mater. 2012;35:718–29.

[27] Nath P, Sarker PK. Effect of GGBFS on setting, workability and early strength properties of fly ash geopolymer concrete cured in ambient condition. Constr Build Mater. 2014;66:163–71.

[28] Al-Rkaby AH. Stabilization of sub-base layers with high gypsum content using lime [dissertation]. Mosul, Iraq: University of Mosul; 2004.

[29] Al-Rkaby AHJ. Evaluating shear strength of sand-GGBFS based geopolymer composite material. Acta Polytech. 2019;59(4):305–11.

[30] Al-Rkaby AH, Chegenizadeh A, Nikraz HR. An experimental study on the cyclic settlement of sand and cemented sand under different inclinations of the bedding angle and loading amplitudes. Eur J Environ Civ Eng. 2019;23(8):971–86.

[31] Al-Rkaby AH, Nikraz HR, Chegenizadeh A. Stress and deformation characteristics of nonwoven geotextile reinforced sand under different directions of principal stress. Int J Geosynth Ground Eng. 2017;3(4):1–11.

[32] Al-Rkaby AH. Strength and deformation of sand-tire rubber mixtures (STRM): an experimental study. Studia Geotech Mech. 2019;41(2):74–80.

[33] Odeh NA, Al-Rkaby AH. Strength, durability, and microstructures characterization of sustainable geopolymer improved clayey soil. Case Stud Constr Mater. 2022:e00988.